Research Square

Preprints are preliminary reports that have not undergone peer review.
They should not be considered conclusive, used to inform clinical practice,
or referenced by the media as validated information.

Decision strategies appear similar across species and development, but differences emerge in the speed-accuracy relationship

Mariella Segreti
Sapienza University of Rome
Sara Dal Sasso
Sapienza University of Rome
Fabio Di Bello
Sapienza University of Rome
Giampiero Bardella
Sapienza University of Rome
Ann Paul
Sapienza University of Rome
Surabhi Ramawat
Sapienza University of Rome
Deny Menghini
Bambino Gesù Children's Hospital
Ferraina Stefano
Sapienza University of Rome
Pierpaolo Pani
Sapienza University of Rome
Emiliano Brunamonti
emiliano.brunamonti@uniroma1.it
Sapienza University of Rome

Article

Keywords:

Posted Date: August 20th, 2026

DOI: https://doi.org/10.21203/rs.3.rs-10499375/v1

License: This work is licensed under a Creative Commons Attribution 4.0 International License.
Read Full License

Additional Declarations: No competing interests reported.

Abstract

Decision-making performance has traditionally been characterized in terms of the speed-accuracy trade-off. One approach to quantifying this relationship is the use of Conditional Accuracy Functions (CAFs). Through CAFs, we investigated decision-making strategies in 62 children, 83 adults, and two macaque monkeys performing a Transitive Inference (TI) task. In all groups, the task elicited the Symbolic Distance Effect, confirming a comparable difficulty-dependent modulation of performance. However, CAF analysis revealed divergent decision-making strategies. Adult humans and monkeys showed similar profiles, whereas children showed a distinct pattern characterized by fast errors. To account for these patterns, we fitted a Drift Diffusion Model (DDM). Performance across species and age groups was explained by a shared computational framework involving difficulty-dependent evidence accumulation and collapsing decision boundaries. However, reproducing the fast errors observed in children required greater variability in the starting point of the decision process. This suggests that, although inferential decision-making mechanisms are evolutionarily conserved, children have less stable initial decision states, likely reflecting the incomplete maturation of frontostriatal networks involved in inhibiting prepotent responses. Combining DDM and CAF frameworks can therefore clarify how decision strategies, developmental stages, and species-specific constraints shape performance, with potential applications to typical development and clinical decision-making impairments.

1. Introduction

Decision-making research typically characterizes performance in terms of how quickly and how accurately choices are made. However, these two dimensions are not independent. In many paradigms, speed and accuracy interact to reach the outcome, giving rise to a speed-accuracy trade-off (SAT), such that faster responses tend to be less accurate, whereas slower responses tend to be more accurate[1–3]. This form of relationship, however, can vary depending on task demands and decision strategy. In some cases, the opposite pattern is observed, with accuracy decreasing at longer response times[4].

Conditional accuracy functions (CAFs) can be used to characterize the relationship between speed and accuracy by estimating accuracy across bins, or quantiles, of the RT distribution[5–7]. CAFs can reveal whether errors are concentrated among the fastest responses, among the slowest ones, or at both ends of the RT distribution[6,8]. Importantly, a fast response does not necessarily indicate that the person knows the answer, just as a slow response does not always reflect careful deliberation. Fast responses may arise from premature commitment, whereas slow responses may reflect either a more prolonged decision process, late uncertainty or even time-pressure-driven responding.

Within this perspective, identifying whether errors are more likely to occur at fast or slow response times can help characterize the strategies that different individuals or populations adopt when approaching a task. For example, evidence from clinical populations shows different CAF patterns, likely reflecting distinct strategies in task performance. Patients with Huntington's disease performing a Simon task[9], for instance, show increased error rates at the fastest response times, consistent with stronger initial

activation of prepotent responses and a greater susceptibility to act on these impulses. This pattern has been linked to changes in fronto-basal ganglia circuits involved in action selection, particularly in medial frontal regions such as the pre-supplementary motor area[10], which may bias the system toward rapid response initiation before sufficient control can be engaged.

In contrast, individuals with ADHD or Tourette syndrome performing a Flanker[11] or Simon task[10] do not consistently exhibit an elevated proportion of fast errors but rather show impairments in suppressing incorrect responses at longer response times[12,13]. This pattern has been interpreted as reflecting reduced efficiency of top-down control mechanisms within frontal-basal ganglia circuitry[13], including the inferior frontal cortex and its interactions with subcortical structures, which are required to suppress incorrect responses after they have been activated. These different outcomes are consistent with the Dual Process Activation-Suppression model[10,13,14], which distinguishes between an early phase of automatic response activation and a later phase of controlled suppression.

Given that frontal networks supporting top-down control undergo maturation during development[15,16] and are more developed in humans than in non-human primates[17], one can ask whether the relationship between speed and accuracy may also vary across age groups and species, for example between children and adults or between humans and non-human primates. To the best of our knowledge, no studies have compared CAF profiles across these groups within the same task. However, it is plausible that they rely on different balances between early response activation and later control processes, giving rise to distinct CAF patterns.

In the present work, we addressed this hypothesis by studying the CAF pattern in a group of 62 children, 83 adult humans and 2 macaque monkeys performing a two-choice decision within the framework of the Transitive inference (TI) task. TI requires the participants to first learn the rank order of arbitrarily defined stimuli, for example, A > B > C > D > E > F, through training on adjacent pairs and are then tested on novel, non-adjacent pairs that require inference from the learned structure[18]. TI tasks elicit a symbolic distance effect (SDE), such that choices become faster and more accurate as the rank distance between the two items increases[18–24]. The SDE has been reported in monkeys and humans, including both children and adults[18,25–29] suggesting the different species rely on comparable abilities that seems to appear early during human development.

Considering that this ability is closely linked to prefrontal cortex function in both humans and monkeys[21,24,30,31], and that full maturation of the prefrontal cortex is reached only in early adulthood[32–35], it is plausible that, beyond the general performance trends observed across non-human primates, children, and adults, a more fine-grained analysis could reveal distinct decision strategies underlying performance on the same task.

By computing the CAF on TI performance, we found that monkeys and adult humans showed a similar approach to the task, whereas children did not. Indeed, children exhibited a stable proportion of fast-

error trials. To interpret these group-specific CAF profiles, we used a Drift Diffusion Model (DDM[36]) to identify the latent decision parameters that best explained the observed behavior. This analysis showed that performance across groups was accounted for by SD-dependent evidence accumulation and a collapsing decision boundary, whereas children with fast errors required an additional source of variability in the starting point of the decision process. This suggests that, although inferential decisions rely on shared computational mechanisms across species and development, children may show less stable initial decision states, leading to premature and poorly informed responses.

2. Methods

2.1. Subjects

The study included 2 adult male rhesus macaques (Macaca mulatta): Monkey 1 (9 years old, 5.50 kg) and Monkey 2 (7 years old, 6.50 kg) at the time of data recording, 83 adults (mean age 25 ± 2.5 years), and 62 children (mean age 10.18 ± 1.16 years). Children were enrolled from 3rd to 6th grade, and school grade corresponded to age in most cases. The mean age was 8.44 ± 0.23 years in 3rd grade, 9.41 ± 0.24 years in 4th grade, 10.72 ± 0.50 years in 5th grade, and 11.40 ± 0.34 years in 6th grade.

Adult participants were healthy volunteers who took part on a voluntary basis. Written informed consent was obtained from all adults in accordance with the protocol approved by the Ethics Committee of the Department of Psychology, Sapienza University of Rome. Child participants were also healthy and were recruited from local primary and secondary schools, in accordance with the Ethics Committee. All participants and their parents gave written informed consent after receiving a comprehensive description of the study.

Animal care, housing, and experimental procedures for the macaques complied with Italian legislation (D.L. 116/92) and European regulations (Directive 2010/63/EU) governing the use of non-human primates in scientific research. The animals were purchased from an authorized supplier and belong to the F2 generation (F2 generation non-human primates). The research protocol was approved by the Italian Ministry of Health (Central Directorate for Veterinary Services). The experiments described in this study were part of a series of experimental procedures planned under the approved protocol, and following the completion of these experiments, the animals were successfully re-introduced into the approved experimental program. Housing conditions and experimental procedures followed the guidelines of the Weatherall report on the use of non-human primates in research.

The datasets analyzed in the present study were all previously published[28,37,38]. In the current work, these datasets were reanalyzed to identify latent parameters that capture similarities and differences across species and age groups in the way the same decision-making task is approached.

2.2. Task structure and stimuli

2.2.1 Experimental task

Each participant completed a TI task with the same conceptual structure. The different groups, however, differed only in the way the chosen options were selected. Each experimental session consisted of a learning phase followed by a test phase.

During the learning phase, participants were required to learn the rank order of six abstract images (A > B > C > D > E > F) by trial and error, comparing pairs of adjacent items (A vs B, B vs C, C vs D, D vs E, E vs F) and indicating the higher-ranking item of the two (Fig. 1A-B).

In children and monkeys, this learning phase comprised two steps: a study phase and a recall phase. During the study phase, each pair was repeatedly presented in blocks of 15 trials for children and 30 trials for monkeys. Each block was repeated until participants achieved at least 80% correct responses for children and 90% for monkeys.

In the recall phase, all adjacent pairs of items were randomly presented (100 trials for both children and monkeys). These blocks were presented until participants met a criterion of 60% correct choices for both children and monkeys. In children, performance at the end of each block was indicated by displaying several smiley faces proportional to their accuracy (≤ 20%, 20–40%, 40–60%, 60–80%, ≥ 80%).

For adult human participants, the learning phase only included blocks of 50 trials with randomly presented adjacent pairs. For these participants, a minimum of 70% correct responses was required to move to the test phase.

In the test phase, all possible pairs of items, both adjacent and non-adjacent, were randomly presented in a block of 150 trials for adults, 150 trials for children, and a variable number of trials for monkeys (approximately 200–400). Adult and child participants each completed a single experimental session, whereas monkeys completed multiple experimental sessions. Specifically, the monkey dataset included 6 sessions for Monkey 1 and 8 sessions for Monkey 2.

In both the learning and test phases, the presentation of the higher-ranking item was counterbalanced between the two possible spatial positions on the screen (top and bottom for adults and children, and left and right for monkeys).

2.2.2 Task time course and experimental setups

At the beginning of each trial, participants maintained their gaze on a fixation spot while holding a predefined starting position. Adults and children fixated the spot for 1 s. During this period, adults kept the joystick in the central position, whereas children placed their index and middle fingers on the lower and upper arrow keys, respectively. Monkeys fixated the spot for 5 s while holding down a red button; if they released the button, the trial was terminated. After the fixation period, the fixation spot was replaced by a pair of items to be compared. Participants were required to indicate the higher-ranking item by moving the joystick (adult task), pressing the corresponding arrow key (children's task), or touching the item on the screen (monkey task). If no response was provided within 2 s of stimulus onset for adults, children, and monkeys, the trial was terminated. Correct and incorrect responses were signaled by

different auditory feedback for human participants, while the correct response in monkeys corresponded to the delivery of a juice reward.

Regarding the monkeys, the analyses were based on 6 sessions for Monkey 1 and 8 sessions for Monkey 2. Macaques completed the task seated in a primate chair positioned in front of a 19-inch touchscreen in a dimly lit room. Stimulus presentation and response recording were controlled using Cortex software (dally.nimh.nih.gov). Animals were free to move their heads and responded by touching the screen. Stimuli were abstract black-and-white images (20° × 20°, equal black-to-white ratio) randomly selected from a pool of 80 stimuli at the beginning of each experimental session.

Adult and children participants were seated approximately 50 cm from a computer screen in a dimly lit room. Stimulus presentation and data acquisition were controlled using Psychtoolbox (www.psychtoolbox.org) in MATLAB (www.mathworks.com). Responses in adults were recorded using a joystick fixed on a table. Children completed the task using the up and down arrow keys on a keyboard. Stimuli were black-and-white images (30 × 30 mm) with an equal black-to-white ratio.

2.4 Behavioral analysis

The proportion of correct responses was computed for each SD level. In both correct and error trials, reaction times (RTs) were computed as the time between pair presentation and response onset, defined as leaving the joystick in the central position in adults, pressing the button in children, and releasing the starting button in monkeys. RT outliers were identified separately for each subject using an interquartile range criterion and were excluded if they fell below Q1−1.5 × IQR or above Q3 + 1.5 × IQR.

For adults and children, analyses were performed at the subject level, as each participant completed a single session. For monkeys, data were aggregated across sessions within each subject before analysis.

As a preliminary analysis, we made sure that accuracy in the final learning block preceding the test phase was significantly above chance in all groups. One learning file from a child was corrupted and could not be opened and was therefore excluded from this analysis; however, performance in that session was above 60% accuracy.

One-way repeated-measures ANOVAs were then performed within each group on accuracy and RTs in correct trials to test if SD significantly modulated these variables.

To further characterize the decision-making process independently of task difficulty related to SD, we examined the relationship between accuracy and response speed. This approach has been previously used to test hypotheses about the processes underlying decision-making and to inform model-based analyses[39]. To do so, we computed conditional accuracy functions (CAFs) by dividing each participant's RT distribution into deciles and calculating accuracy within each bin[7], defined as the proportion of correct trials relative to the total number of trials in that bin. Then, we assessed whether fast and slow errors were equally distributed within each group. Following the terminology used by Kang and colleagues[8], we defined fast and slow errors according to their position within the RT distribution, with

fast errors occurring at the shortest RTs and slow errors at the longest RTs. To operationalize this distinction, we mathematically identified participants or sessions characterized by fast and slow errors by applying a bin-based criterion to the CAFs. For each participant, mean accuracy and standard deviation were calculated across intermediate RT bins (from 3 to 7). Accuracy in the earliest bins (1 and 2) was then compared against this reference distribution. A participant or session met the fast-error criterion if accuracy in either of the first two bins was at least one standard deviation below the mean of bins 3–7 and also fell below an absolute threshold of 80%. Bins 3–7 were selected as a reference because they correspond to the central portion of the RT distribution and are less likely to be influenced by slow errors.

For slow errors, accuracy in the latest bins (from 8 to 10) was compared against the same reference distribution. Once again, a participant or session met the slow-error criterion if accuracy in at least one of the last three bins decreased by at least one standard deviation relative to the mean accuracy of the central bins.

Given the presence of fast errors in children, but not in adults and monkeys (see Results), we further subdivided the children group based on the occurrence of fast errors.

All statistical analyses were performed in MATLAB2023b (MathWorks Inc., 2023; www.mathworks.com) and Python 3.13 (Python Release Python 3.13.0 | Python.org; specifically, using statsmodels[40]) with the threshold for statistical significance set at $\alpha = 0.05$. When the repeated measures ANOVAs were significant, pairwise Fisher's LSD post hoc comparisons were performed.

2.5. Modeling

To uncover latent variables underlying pairwise comparisons and the studied decision-making process, trial-level choice and RT data were fitted with a set of DDMs[36]. Prior to model fitting, RT outlier trials were removed using the same procedure described above. Model fitting was carried out in PyDDM[41], a Python library that provides built-in functions for estimating DDM parameters.

Within this framework, several parameters can be estimated: the drift rate, which reflects the rate of evidence accumulation[36]; the boundary, representing the amount of evidence required before committing to a decision[36]; the starting point (z), which is the initial state of the decision process[8]; and the non-decision time (NDT), which captures processes occurring outside evidence accumulation, such as sensory encoding[42].

For each subject and session, we tested different versions of DDM by systematically varying different model parameters. A graphical representation of the different models' architectures is provided in Fig. 2. First, we implemented a null model (Fig. 2a), in which all parameters were held constant across SD. This model served as a control for assessing whether SD improved the explanatory power of the fit. Beyond the null model, several models were tested:

1. SD-dependent drift model (Fig. 2b): drift parameterized as a function of SD, while boundary remained fixed[37,43].

$$drift_{SD} = drift_{0} + \beta \times SD$$

where $drift_0$ represents the baseline rate of evidence accumulation, and β captures how strongly the drift rate increases as a function of SD.

2. SD-dependent drift and collapsing model (Fig. 2c): drift was modeled as a linear function of SD, and boundary as a collapsing function of time (t), following the methodology of Munoz and colleagues[26].

$$drift_{SD} = drift_{0} + \beta \times SD$$

$$boundary(t) = boundary_{0} \exp(-t/tau)$$

where $boundary_0$ is the initial boundary separation and tau controls the rate at which the boundary collapses.

3. SD-dependent drift, collapsing, and z variability model (Fig. 2d): in order to account for all possible strategies adopted during the decision-making task, including the occurrence of fast error trials, that is, choices made at a very early stage of the trial, we introduced an additional version of the DDM incorporating trial-by-trial z variability[8,44]. As noted in the methodological recommendations of Boehm and colleagues[44], z variability should be estimated only when there is clear evidence of fast errors in the data. For this reason, we tested this model extension only in a subset of children (see Results section), as they were the only group showing the presence of fast errors.

$$drift_{SD} = drift_{0} + \beta \times SD$$

$$boundary(t) = boundary_{0} \exp(-t/tau)$$

$$z \sim Uniform(z - sz/2, z + sz/2)$$

where z represents the mean starting point of the decision process, and sz defines the range of across-trial variability around this mean. On each trial, z is sampled from a uniform distribution over the interval [z − sz/2, z + sz/2], such that all values within this range are equally likely. Although the distribution is uniform, its position is determined by z: when z is shifted toward one of the decision boundaries, a larger proportion of starting points lie closer to that boundary, introducing a response bias. As a result, the accumulation process can begin from different initial states across trials, with some trials starting closer to the error boundary and thus more likely to produce fast errors[8].

By computing the Akaike Information Criterion (AIC[45,46]) for each subject and monkey session, we then identified the model variant that provided the best fit to the observed data, as indicated by the lowest AIC value[45–47].

All model analyses were performed in Python 3.13 (Python Release Python 3.13.0 | Python.org) using statsmodels[40] with the threshold for statistical significance set at $\alpha = 0.05$.

3. Results

3.1. Symbolic distance modulates accuracy and reaction times in adult humans, children, and monkeys

We first evaluated if all groups properly learned the task by testing accuracy in the final learning block preceding the test phase. Accuracy was significantly above chance in all groups. Adults showed high accuracy (90.55 ± 4.54), $t(82) = 81.37$, $p = 3.43 \times 10^{-80}$. Children also performed above chance (70.59 ± 7.76), $t(60) = 20.73$, $p = 4.85 \times 10^{-29}$. Similarly, both monkeys showed above-chance performance: Monkey 1 (96.52 ± 2.03), $t(5) = 56.07$, $p = 3.41 \times 10^{-8}$, and Monkey 2 (72.39 ± 5.06), $t(7) = 12.52$, $p = 4.78 \times 10^{-6}$.

These results indicate the correct acquisition of the adjacent pairs' reciprocal ordinal relation.

The analysis of the test phase showed that all groups were able to compare non-adjacent pairs. In fact, performance varied as a function of SD, with both accuracy and RT showing clear modulation across SD levels (Fig. 3A-B).

Consistent with this pattern, one-way ANOVAs within each group confirmed a significant main effect of SD on both accuracy and RT (Table 1). Post hoc analyses further indicated that, in every group, performance differed across multiple SD levels, with a broad pattern of significant pairwise differences summarized in Supplementary Fig. 1.

Table 1
One-way repeated-measures ANOVAs with SD as factor.

Group	Outcome	F(df1, df2)	p
Monkey 1	Accuracy	F(4, 20) = 45.68	8.8×10^{-10}
Monkey 2	Accuracy	F(4, 28) = 34.56	1.9×10^{-10}
Adults	Accuracy	F(4, 328) = 82.49	2.2×10^{-48}
Children	Accuracy	F(4, 244) = 91.35	2.4×10^{-47}
Monkey 1	RT (ms)	F(4, 20) = 19.19	1.3×10^{-6}
Monkey 2	RT (ms)	F(4, 28) = 24.65	8.0×10^{-9}
Adults	RT (ms)	F(4, 328) = 177.01	1.4×10^{-80}
Children	RT (ms)	F(4, 244) = 37.36	2.3×10^{-24}

3.2. Group-specific speed-accuracy strategies and their developmental modulation

After establishing that SD shaped performance in each group, we examined if this pattern reflected group-specific strategies in pair comparisons or whether it was consistent across individuals. To address this question, we first assessed if fast and slow errors were equally distributed within each group (Supplementary Fig. 2), finding that, in adult humans, children, and monkeys, the proportion of errors increased with longer RT. However, the distribution showed a visible presence of fast errors only in children.

We therefore examined the CAFs (Fig. 4A) to quantify this pattern and applied the fast- and slow-error criteria described in the Methods. Slow errors were broadly distributed across groups, occurring in 63 out of 83 adults (75.9%), 35 out of 62 children (56.5%), 6 out of 6 Monkey 1's sessions (100%), and 8 out of 8 Monkey 2's sessions (100%).

Instead, although the RT-error distribution showed a presence of fast errors in children (Supplementary Fig. 2), the bin-based criterion indicated that this pattern was driven by a subset of participants. Specifically, 26 out of 62 children (41.9%) met the fast-error criterion. In addition, no adults (0 out of 83) or monkey sessions (0 out of 14) met the fast-error criterion (see Methods). Based on this classification, we further divided the children into two subgroups: fast error children (Children FE) and no fast error children (Children NFE), and examined their CAFs separately (Fig. 4A). Children FE exhibited an inverted U-shaped relationship between RT and accuracy, with lower accuracy for both the fastest and slowest responses and higher accuracy at intermediate RTs. By contrast, children NFE showed no clear modulation of accuracy across RT bins.

For a more in-depth analysis, we computed, separately for each group, the CAF for each SD to determine whether slow errors were concentrated at smaller SDs, eliciting longer RTs, or were spread across all distances. We applied the same analysis to the distribution of fast errors (Fig. 4B).

Using two-way repeated-measures ANOVAs with RT bin and SD as factors, we found a main effect of SD in each group and a main effect of RT bin in adults, monkeys, and children FE, but not in children NFE (Table 2). We detected a significant interaction between RT bin and SD only in adult humans.

Table 2
Two-way repeated-measures ANOVAs with RT bin and SD as factors.

Group	Outcome	$F(df_1, df_2)$	p
Adults	SD	$F(4, 328) = 39.44$	1.1×10^{-16}
	RT bin	$F(9, 738) = 25.73$	1.1×10^{-16}
	SD × RT bin	$F(36, 2952) = 3.19$	6.0×10^{-10}
Monkey 1	SD	$F(4, 20) = 15.23$	7.3×10^{-6}
	RT bin	$F(9, 45) = 11.44$	4.6×10^{-9}
	SD × RT bin	$F(36, 180) = 1.25$	.176
Monkey 2	SD	$F(4, 28) = 20.90$	4.5×10^{-8}
	RT bin	$F(9, 63) = 4.08$	.0004
	SD × RT bin	$F(36, 252) = 1.36$	.095
Children FE	SD	$F(4, 100) = 47.79$	1.1×10^{-16}
	RT bin	$F(9, 225) = 12.01$	2.0×10^{-15}
	SD × RT bin	$F(36, 900) = 1.24$	.161
Children NFE	SD	$F(4, 140) = 47.66$	1.1×10^{-16}
	RT bin	$F(9, 315) = 0.65$	.756
	SD × RT bin	$F(36, 1260) = 1.41$	.055

Post-hoc analysis of SD levels highlighted, in each group, significantly higher accuracy for larger SDs across the CAF distribution, regardless of the RT bin (see details of comparisons in Supplementary Fig. 3).

The analysis of post-hoc comparisons on RT bin (Supplementary Fig. 2) indicated that, in adults, significant differences were mainly driven by contrasts involving the slowest RT bins (B8-B10). A similar pattern was observed in monkeys. In children FE, a different pattern was found: the earliest bin (B1-2) differed significantly from the majority of the other bins, while the slowest bin (B10) significantly differed from the central ones (B5-6).

Finally, we investigated a possible developmental effect on the CAF pattern by quantifying the proportion of children FE across school grades (3rd to 6th grade; Fig. 4B). Although the proportion of children FE was lower in 6th grade (19%) compared with earlier grades (42% in 3rd grade, 54% in 4th grade, 52% in 5th grade), this difference did not reach statistical significance ($\chi^2(3) = 5.23$, $p = 0.156$). Nevertheless, the observed pattern is consistent with a gradual reduction of fast errors across development, in line with their absence in adult participants.

3.3. Drift dynamics and boundary collapse account for inferential decisions across species and ages, with children requiring additional starting-point variability

To identify the latent decision variables underlying TI performance, we fitted trial-level choice and RT data with a set of DDMs and compared model fits using AIC. We observed that in adults, children NFE, and monkeys, the SD-dependent drift and collapsing model provided the best account of the data in nearly all sessions and subjects. Figure 5A illustrates that this version of the model returned the lowest AIC values, indicating higher goodness of fit (blue raincloud plots). The only exception was 1 out of 83 adult participants, for whom the drift-only model provided a better fit. In children FE, we introduced a model with an additional parameter, z variability, which provided the best goodness of fit in the vast majority of children in this group (23 out of 26).

Together, the parameter estimates included NDT (Fig. 5B), drift rate as a function of SD (Fig. 5C), and the tau parameter controlling the collapse of the decision boundary over time (Fig. 5D, E). Thereby, in all groups, drift rate systematically varied as a function of SD, and the decision boundary showed a collapse over time.

To visualize the decision processes implied by the SD-dependent drift and collapsing model, as well as the SD-dependent drift, collapsing, and z-variability model, we then generated latent decision-variable trajectories using subject-specific parameter estimates. For two example children with different best-fitting models, 150 trials were simulated by allowing the decision variable to evolve over time according to the fitted drift, noise, and decision boundaries until one of the two boundaries was reached. When included in the fitted model, z variability was also used to initialize the simulated trajectories.

For both example subjects, simulated trials were grouped into correct responses, fast errors, and other errors. Errors were classified using the same equinumerous RT bins adopted for the CAF analysis, with 10 bins per subject. Fast errors were defined as error trials falling within the two fastest RT bins, whereas other errors comprised the remaining error trials. As expected, inspection of single-trial latent trajectories showed that, in the model including z variability, fast errors were preferentially associated with trajectories starting closer to the incorrect boundary (Fig. 6A). By contrast, such fast errors were essentially absent in the model without z variability (Fig. 6B).

4. Discussion

In the present study, we adopted a comparative approach across multiple groups to investigate potential developmental differences in decision strategies in a memory schema-driven task. To this end, we employed a TI task, which is a complex cognitive task and is therefore expected to predominantly elicit slow errors[48].

Before examining differences in error dynamics, we first verified that the typical behavioral signatures of TI were present across groups. In line with previous findings in children[28,49], adults[37], and non-human primates[26,50], the SDE shaped the behavioral outcomes in all groups. This confirmed that task difficulty

affected performance similarly across groups and that participants in each group approached the task with comparable cognitive strategies[18].

However, previous studies have shown that task difficulty is not the only factor modulating accuracy[5,48,51]. For example, even when the level of difficulty is held constant in perceptual decision-making tasks[4,39], contextual factors such as emphasis on accuracy or pressure to respond can promote different types of errors. When speed is emphasized[52–55], a higher proportion of errors tends to occur at very short RT, reflecting the prioritization of responding over proper analysis of the available information[48,51]. This type of error is referred to as “fast errors”[51,56] and is typically interpreted as resulting from the execution of prepotent action impulses that are insufficiently inhibited[48]. In contrast, when accuracy is emphasized, errors are more likely to occur at longer RT, often reflecting reduced sustained attention and higher decision uncertainty[48,57], and are more commonly observed in cognitively demanding conditions[48,57].

In the present work, we did not systematically manipulate the priority to the speed or the accuracy of the response. However, the instruction to be as accurate as possible placed both adult and young human participants in a context where accuracy was prioritized. We placed the monkeys in a comparable condition by rewarding each monkey's correct choice and providing them with sufficient time to respond. Considering this framework, it was expected to observe in each group of participants a general decrease of the accuracy associated with the increasing of the RT. This pattern was observed in the majority of participants, who showed lower accuracy in at least one of the last three RT deciles. In addition, as expected[48], slow errors in adult humans were mainly associated with difficult conditions. However, children and monkeys also exhibited slow errors in easier conditions, suggesting the adoption of a different decision-making strategy.

Surprisingly, a subset of children also displayed a significant proportion of fast errors. This pattern is consistent with the idea that children may produce fast guesses, that is, responses initiated before sufficient relational evidence has been accumulated[58]. Indeed, as shown in Fig. 4B, accuracy in the first RT bin is close to chance level, indicating that these early responses are only weakly informed by the relational structure of the task. This finding is in line with previous work suggesting that, when task demands exceed their capacities, children may produce rapid and partly random responses[59]. A plausible explanation for this pattern could be that, despite the priority on accuracy, children could have a tendency to respond impulsively, suggesting a lower degree of behavioral control.

Interestingly, fast errors were distributed across the different levels of difficulty (represented here by the SD), suggesting a general approach to task solving beyond difficulty-related performance.

The present results support the view that developmental CAF profiles in cognitive tasks may provide a framework for understanding psychiatric and neurodegenerative conditions characterized by distinct distributions of fast and slow errors. Indeed, evidence from clinical populations such as Huntington

disease, ADHD, and Tourette syndrome[10,12,13], indicates that different CAF profiles reflect variations in underlying cognitive processes. In addition, our findings support the hypothesis of a changed relationship between speed and accuracy based on age and species, in agreement with the maturation during development of top-down control from frontal networks[15,16] and with the fact that this network is more developed in humans than in non-human primates[17].

However, although these profiles describe how errors are distributed across the RT distribution, they do not directly identify the latent decision processes generating them. We therefore complemented the behavioral analyses with DDM, which is widely used to uncover the computational processes underlying decision-making from observed behavioral outcomes[60,61].

To account for patterns observed in CAF and SAT studies, the classical DDM with fixed decision boundaries was extended to incorporate urgency and impatience. This led to collapsing-boundary models, in which the amount of evidence required to produce a response progressively decreases over time[62,63]. In these models, as the boundaries collapse, weak or noisy evidence becomes increasingly likely to trigger a response, potentially accounting for the slow errors observed in the later portion of the RT distribution[62,64]. The higher error rate arises because, when the boundaries are closer together, even small stochastic fluctuations can drive the decision variable toward either the correct or the incorrect boundary[65].

Consistent with the mechanism described above, our modelling results showed that performance was jointly shaped by evidence accumulation and boundary dynamics. Specifically, in line with previous findings[26,37,43], we found that the difficulty-related drift rate is a primary variable underlying task performance. In addition, models with collapsing boundaries provided a better account of the data than models with fixed boundaries. In our paradigm, the cost structure favors responding rather than waiting and may therefore promote boundary collapse. Indeed, failures to respond within the time limit are scored as incorrect trials. Under these conditions, committing to a choice preserves some probability of success even when the accumulated evidence is weak. This may increase urgency over time, progressively reducing the amount of evidence required to respond. In monkeys, this tendency may be further strengthened by reward contingencies, because responding within the available time window allows earlier access to juice even under uncertainty[66].

These results also highlight the relevance of collapsing boundary dynamics. In fact, the collapse parameter tau may provide an index of individual differences in decision strategy. Individuals with a more impulsive decision style would be expected to exhibit a steeper boundary collapse, reflected by smaller tau values, whereas individuals characterized by excessive caution, such as those with obsessive-compulsive traits[67], may show a slower collapse, reflected by larger tau values, or no evidence of boundary collapse.

However, the above-mentioned parameters were not sufficiently powerful to account for the fast errors observed in children, suggesting that additional parameters may need to be considered when modelling

decision-making in different populations. One possible explanation is that children are more susceptible to trial-to-trial fluctuations in cognitive state, such as variations in attentional engagement or focus, which may increase the likelihood of early, poorly informed responses.

Previous work has modelled these fluctuations as trial-to-trial variability in the starting point z[68]. Greater variability in z increases the likelihood that some decisions begin closer to the incorrect boundary, producing fast errors before sufficient evidence has been accumulated[44]. Consistent with this interpretation, Turner and colleagues[68] showed that trial-to-trial changes in neural activity in task-relevant regions, including the orbitofrontal cortex, can influence behaviour, even when task demands remain constant.

Although the present study did not include neural measurements and this interpretation therefore remains speculative, our findings are consistent with this account. In particular, the model including z variability provided the best goodness-of-fit for the children FE group, supporting the possibility that fast errors in this group may reflect greater fluctuations in cognitive state across trials.

From a comparative and developmental perspective, these results suggest that, while the computational parameters underlying the ability to make inferences is highly conserved across primates and developmental stages, the ability to stabilize the initial state of a decision and inhibit prepotent impulses is a protracted maturation process, likely reflecting the refinement of fronto-striatal networks across the lifespan.

Finally, these findings may have clinical relevance, given that DDM parameters have already helped clarify the mechanisms underlying decision-making alterations in clinical and developmental populations, including autism spectrum conditions[69], ADHD[70,71], schizophrenia[72], and aging[73–75].

Declarations

Author Contributions Statement

M.S., S.D.S., F.D.B., A.P., and E.B. curated the data. M.S., S.D.S. and E.B. performed the formal analysis. M.S., S.D.S., and A.P. prepared the figures. P.P., S.F., and E.B. conceptualized the study.

E.B. conducted the investigation. M.S., S.D.S., F.D.B., G.B., D.M., P.P., S.F. and E.B. developed methodology. S.F., P.P., and E.B. administered the project. S.F. and D.M. provided resources.

P.P. and E.B. supervised the study. M.S., S.D.S. and E.B. wrote the original draft. All authors reviewed and edited the manuscript.

Competing Interests Statement

The authors declare no competing interests.

Funding

Italian Ministry of University and Research, Program PRIN 2022.

Data Availability

After publication, the script used for the DDM modeling will be made available in an open repository, while the original data will be available upon reasonable request.

References

1. Donkin, C., Little, D. R. & Houpt, J. W. Assessing the speed-accuracy trade-off effect on the capacity of information processing. *J. Exp. Psychol. Hum. Percept. Perform.* **40**, 1183–1202 (2014).
2. Spieser, L., Servant, M., Hasbroucq, T. & Burle, B. Beyond decision! Motor contribution to speed–accuracy trade-off in decision-making. *Psychon Bull. Rev.* **24**, 950–956 (2017).
3. Martínez, A., Blanch, A. & Age Skill, and the Speed-Accuracy Trade-off With a Recall Task in Chess. *Percept. Mot Skills* **40**, (2026).
4. Murphy, P. R., Boonstra, E. & Nieuwenhuis, S. Global gain modulation generates time-dependent urgency during perceptual choice in humans. *Nat. Commun.* **7**, (2016).
5. Heitz, R. P. The speed-accuracy tradeoff: history, physiology, methodology, and behavior. *Front. Neurosci.* **8**, (2014).
6. van Maanen, L., Katsimpokis, D. & van Campen, A. D. Fast and slow errors: Logistic regression to identify patterns in accuracy–response time relationships. *Behav. Res. Methods*. **51**, 2378–2389 (2019).
7. Ponce, R., Lupiáñez, J., González-García, C., Casagrande, M. & Marotta, A. Exploring the spatial interference effects elicited by social and non-social targets: A conditional accuracy function approach. *Br. J. Psychol.* **116**, 69–88 (2025).
8. Kang, I., De Boeck, P. & Ratcliff, R. Modeling Conditional Dependence of Response Accuracy and Response Time with the Diffusion Item Response Theory Model. *Psychometrika* **87**, 725–748 (2022).
9. Simon, J. R. Reactions toward the source of stimulation. *J. Exp. Psychol.* **81**, 174–176 (1969).
10. Shiino, S., van Wouwe, N. C., Wylie, S. A., Claassen, D. O. & McDonell, K. E. Huntington disease exacerbates action impulses. *Front. Psychol.* **14**, (2023).
11. Eriksen, B. A. & Eriksen, C. W. Effects of noise letters upon the identification of a target letter in a nonsearch task. *Percept. Psychophys*. **16**, 143–149 (1974).
12. Ridderinkhof, K. R., Scheres, A., Oosterlaan, J. & Sergeant, J. A. Delta Plots in the Study of Individual Differences: New Tools Reveal Response Inhibition Deficits in AD/HD That Are Eliminated by Methylphenidate Treatment. *J. Abnorm. Psychol.* **114**, 197–215 (2005).

13. Wylie, S. A., Claassen, D. O., Kanoff, K. E., Ridderinkhof, K. R. & van den Wildenberg, W. P. M. Impaired inhibition of prepotent motor actions in patients with Tourette syndrome. *J. Psychiatry Neurosci.* **38**, 349–356 (2013).
14. van den Wildenberg, W. P. M. et al. To Head or to Heed? Beyond the Surface of Selective Action Inhibition: A Review. *Front. Hum. Neurosci.* **4**, (2010).
15. Hwang, K. & Luna, B. The Development of Brain Connectivity Supporting Prefrontal Cortical Functions. in Principles of Frontal Lobe Function 164–184 (Oxford University Press, doi:10.1093/med/9780199837755.003.0014. (2013).
16. Walhovd, K. B. et al. Maturation of Cortico-Subcortical Structural Networks–Segregation and Overlap of Medial Temporal and Fronto-Striatal Systems in Development. *Cereb. Cortex*. **25**, 1835–1841 (2015).
17. Barrett, R. L. C. et al. Differences in Frontal Network Anatomy Across Primate Species. *J. Neurosci.* **40**, 2094–2107 (2020).
18. Ramawat, S. et al. The transitive inference task to study the neuronal correlates of memory-driven decision making: A monkey neurophysiology perspective. *Neurosci. Biobehav Rev.* **152**, 105258 (2023).
19. Wu, X. & Levy, B. W. Simulating symbolic distance effects in the transitive inference problem. *Neurocomputing* **38**, (2001).
20. Acuna, B. D. Frontal and Parietal Lobe Activation during Transitive Inference in Humans. *Cereb. Cortex*. **12**, 1312–1321 (2002).
21. Brunamonti, E. et al. Neuronal Modulation in the Prefrontal Cortex in a Transitive Inference Task: Evidence of Neuronal Correlates of Mental Schema Management. *J. Neurosci.* **36**, 1223–1236 (2016).
22. Mione, V., Brunamonti, E., Pani, P., Genovesio, A. & Ferraina, S. Dorsal Premotor Cortex Neurons Signal the Level of Choice Difficulty during Logical Decisions. *Cell. Rep.* **32**, 107961 (2020).
23. Markant, D. B. Active transitive inference: When learner control facilitates integrative encoding. *Cognition* **200**, 104188 (2020).
24. Ramawat, S. et al. Different Contribution of the Monkey Prefrontal and Premotor Dorsal Cortex in Decision Making During a Transitive Inference Task. *Neuroscience* **485**, 147–162 (2022).
25. D'Amato, M. R. & Colombo, M. The symbolic distance effect in monkeys (Cebus apella). *Anim. Learn. Behav.* **18**, 133–140 (1990).
26. Munoz, F. et al. Learning Decouples Accuracy and Reaction Time for Rapid Decisions in a Transitive Inference Task. *J. Cogn. Neurosci.* **38**, (2026).
27. Gazes, R. P., Hampton, R. R. & Lourenco, S. F. Transitive inference of social dominance by human infants. *Dev. Sci.* **20**, (2017).
28. Brunamonti, E. et al. Evaluation of relational reasoning by a transitive inference task in attention-deficit/hyperactivity disorder. *Neuropsychology* **31**, (2017).

29. Gazes, R. P. & Lazareva, O. F. Does cognition differ across species, and how do we know? Lessons from research in transitive inference. *J. Exp. Psychol. Anim. Learn. Cogn.* **47**, 223–233 (2021).
30. Koscik, T. R. & Tranel, D. The Human Ventromedial Prefrontal Cortex Is Critical for Transitive Inference. *J. Cogn. Neurosci.* **24**, (2012).
31. Di Bello, F., Mione, V., Pani, P., Brunamonti, E. & Ferraina, S. Prefrontal cortex contribution in transitive inference task through the interplay of beta and gamma oscillations. *Commun. Biol.* **7**, (2024).
32. Casey, B., Galvan, A. & Hare, T. A. Changes in cerebral functional organization during cognitive development. *Curr. Opin. Neurobiol.* **15**, (2005).
33. Tsujimoto, S. The Prefrontal Cortex: Functional Neural Development During Early Childhood. *Neuroscientist* **14**, (2008).
34. Spencer-Smith, M. & Anderson, V. Healthy and abnormal development of the prefrontal cortex. *Dev. Neurorehabil* **12**, (2009).
35. Forde, N. J. et al. Healthy cortical development through adolescence and early adulthood. *Brain Struct. Funct.* **222**, (2017).
36. Ratcliff, R. & McKoon, G. The Diffusion Decision Model: Theory and Data for Two-Choice Decision Tasks. *Neural Comput.* **20**, (2008).
37. Paul, A. et al. Individual differences in learning and decision-making: the role of COMT Val158Met polymorphism in transitive inference. *Exp. Brain Res.* **244**, (2026).
38. Brunamonti, E. et al. The NMDAr antagonist ketamine interferes with manipulation of information for transitive inference reasoning in non-human primates. *J. Psychopharmacol.* **28**, (2014).
39. Standage, D., Blohm, G. & Dorris, M. C. On the neural implementation of the speed-accuracy trade-off. *Front. Neurosci.* **8**, (2014).
40. Seabold, S. & Perktold, J. Statsmodels: econometric and statistical modeling with python. in (2010).
41. Shinn, M., Lam, N. H. & Murray, J. D. A flexible framework for simulating and fitting generalized drift-diffusion models. *Elife* **9**, (2020).
42. Carpio, A., Fernandes-Magalhaes, R., Ferrera, D. & de Lahoz, M. E. Drift Diffusion Models as an Interpretable Framework for Modeling Decision-Making Behavior. in Computational and Deep Learning Models for Advanced Behavioral Analysis 391–424IGI Global Scientific Publishing, (2026). 10.4018/979-8-3373-5062-2.ch012
43. Marc, I. B. et al. The Difficulty in Numerical Computation Impacts Motor Decisions in a Stop-Signal Task. *Eur. J. Neurosci.* **63**, (2026).
44. Boehm, U. et al. Estimating across-trial variability parameters of the Diffusion Decision Model: Expert advice and recommendations. *J. Math. Psychol.* **87**, (2018).
45. Akaike, H. A new look at the statistical model identification. *IEEE Trans. Automat Contr*. **19**, 716–723 (1974).
46. Akaike, H. Akaike's Information Criterion. in International Encyclopedia of Statistical Science 41–42 (Springer Berlin Heidelberg, Berlin, Heidelberg, doi:10.1007/978-3-662-69359-9_14. (2025).

47. Burnham, K. P. & Anderson, D. R. Advanced Issues and Deeper Insights. in Model Selection and Multimodel Inference: A Practical Information-Theoretic Approach (eds Burnham, K. P. & Anderson, D. R.) 267–351 (Springer New York, New York, NY, doi:10.1007/978-0-387-22456-5_6. (2002).
48. Novikov, N. A. et al. Slow and Fast Responses: Two Mechanisms of Trial Outcome Processing Revealed by EEG Oscillations. *Front. Hum. Neurosci.* **11**, (2017).
49. Kao, T., Michaelcheck, C., Ferrera, V. P., Terrace, H. S. & Jensen, G. Transitive inference in a clinical childhood sample with a focus on autism spectrum disorder. *Autism Res.* **17**, (2024).
50. Marc, I. B. et al. Dynamics of oscillatory power support the integration of perceptual and mnemonic information within the premotor cortex. *Nat. Commun.* **17**, (2026).
51. Matzke, D., Curley, S., Gong, C. Q. & Heathcote, A. Inhibiting responses to difficult choices. *J. Exp. Psychol. Gen.* **148**, (2019).
52. Verbruggen, F. & Logan, G. D. Response inhibition in the stop-signal paradigm. *Trends Cogn. Sci.* **12**, (2008).
53. Albert, J. et al. The development of selective stopping: Qualitative and quantitative changes from childhood to early adulthood. *Dev. Sci.* **25**, (2022).
54. Haque, M. T. et al. Attentional spatial cueing of the stop-signal affects the ability to suppress behavioural responses. *Exp. Brain Res.* **242**, (2024).
55. Haque, M. T. et al. Inhibition of return emerges with non-predictive spatial cueing of the stop-signal. *Front. Hum. Neurosci.* **19**, (2025).
56. Ratcliff, R. & Rouder, J. N. Modeling Response Times for Two-Choice Decisions. *Psychol. Sci.* **9**, (1998).
57. van Driel, J., Ridderinkhof, K. R. & Cohen, M. X. Not All Errors Are Alike: Theta and Alpha EEG Dynamics Relate to Differences in Error-Processing Dynamics. *J. Neurosci.* **32**, (2012).
58. Dutilh, G., Wagenmakers, E. J., Visser, I. & van der Maas, H. L. J. A Phase Transition Model for the Speed-Accuracy Trade-Off in Response Time Experiments. *Cogn. Sci.* **35**, (2011).
59. Bolsinova, M., Tijmstra, J. & Molenaar, D. Response moderation models for conditional dependence between response time and response accuracy. *Br. J. Math. Stat. Psychol.* **70**, (2017).
60. Harris, A. & Hutcherson, C. A. Temporal dynamics of decision making: A synthesis of computational and neurophysiological approaches. *Wires Cogn. Sci.* **13**, (2022).
61. Yee, D. M. Neural and Computational Mechanisms of Motivation and Decision-making. *J. Cogn. Neurosci.* **36**, (2024).
62. Boehm, U., Hawkins, G. E., Brown, S., van Rijn, H. & Wagenmakers, E. J. Of monkeys and men: Impatience in perceptual decision-making. *Psychon Bull. Rev.* **23**, (2016).
63. Kelly, S. P., Corbett, E. A. & O'Connell, R. G. Neurocomputational mechanisms of prior-informed perceptual decision-making in humans. *Nat. Hum. Behav.* **5**, (2021).
64. Voskuilen, C., Ratcliff, R. & Smith, P. L. Comparing fixed and collapsing boundary versions of the diffusion model. *J. Math. Psychol.* **73**, (2016).

65. Myers, C. E., Interian, A. & Moustafa, A. A. A practical introduction to using the drift diffusion model of decision-making in cognitive psychology, neuroscience, and health sciences. *Front. Psychol.* **13**, (2022).
66. Karşılar, H., Simen, P., Papadakis, S. & Balcı, F. Speed accuracy trade-off under response deadlines. *Front. Neurosci.* **8**, (2014).
67. Abramowitz, J. S. et al. Enhancing Exposure and Response Prevention for OCD: A Couple-Based Approach. *Behav. Modif.* **37**, 189–210 (2013).
68. Turner, B. M., van Maanen, L. & Forstmann, B. U. Informing cognitive abstractions through neuroimaging: The neural drift diffusion model. *Psychol. Rev.* **122**, (2015).
69. Pirrone, A., Dickinson, A., Gomez, R., Stafford, T. & Milne, E. Understanding perceptual judgment in autism spectrum disorder using the drift diffusion model. *Neuropsychology* **31**, (2017).
70. Metin, B. et al. ADHD performance reflects inefficient but not impulsive information processing: A diffusion model analysis. *Neuropsychology* **27**, (2013).
71. Shapiro, Z. & Huang-Pollock, C. A diffusion-model analysis of timing deficits among children with ADHD. *Neuropsychology* **33**, (2019).
72. Moustafa, A. A. et al. Drift diffusion model of reward and punishment learning in schizophrenia: Modeling and experimental data. *Behav. Brain. Res.* **291**, (2015).
73. Ratcliff, R., Thapar, A. & Mckoon, G. A diffusion model analysis of the effects of aging on brightness discrimination. *Percept. Psychophys* **65**, (2003).
74. Ratcliff, R., Thapar, A. & McKoon, G. A diffusion model analysis of the effects of aging on recognition memory. *J. Mem. Lang.* **50**, (2004).
75. Theisen, M., Lerche, V., von Krause, M. & Voss, A. Age differences in diffusion model parameters: a meta-analysis. *Psychol. Res.* **85**, (2021).

Figures

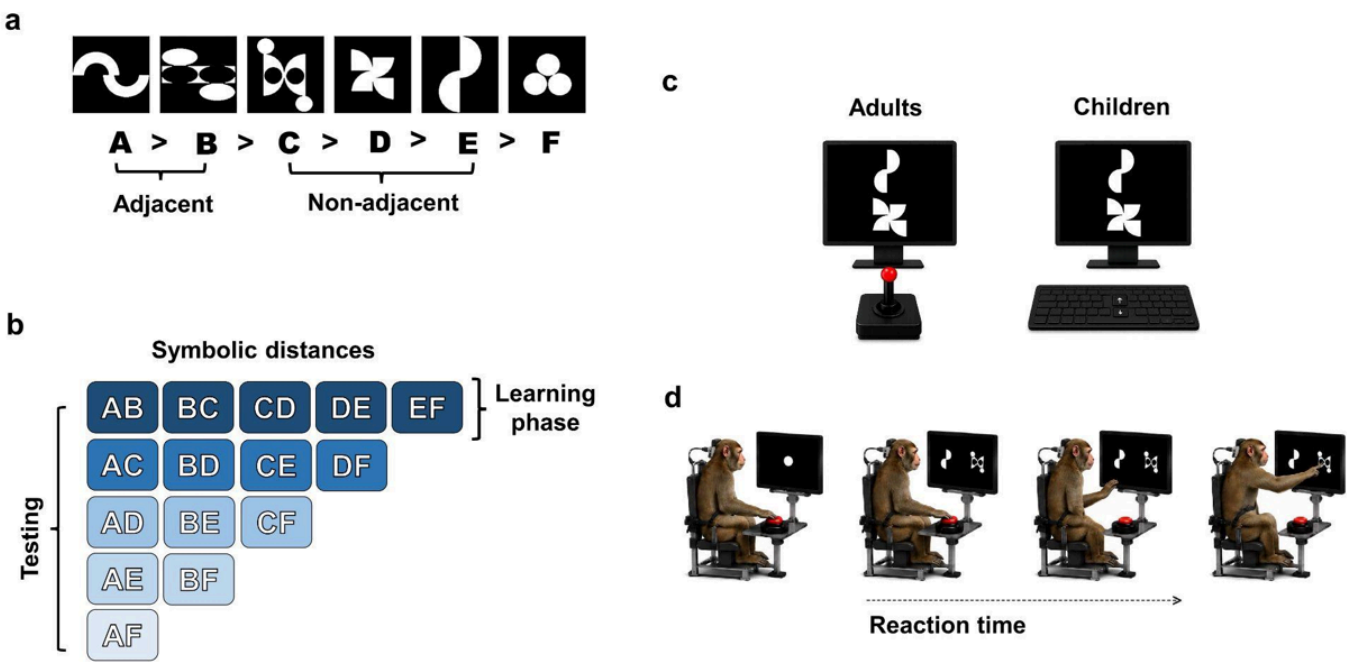


Figure 1

Transitive Inference (TI) task. **a**. Sample of a set of items arranged in a ranked order. Adjacent item pairs were used during the learning phase, while non-adjacent pairs were used in the testing phase. **b.** Symbolic distances (SDs) and pair combinations. In the testing phase, each SD level, from SD1 to SD5, included 15 different item pairs. For each trial, the target item appeared randomly in either the upper or lower position. In the Test Phase, the rule followed the order A > B through E > F. **c**. Trial structure and response modalities across species and age groups. Each trial consisted of fixation, pair presentation, and response selection.

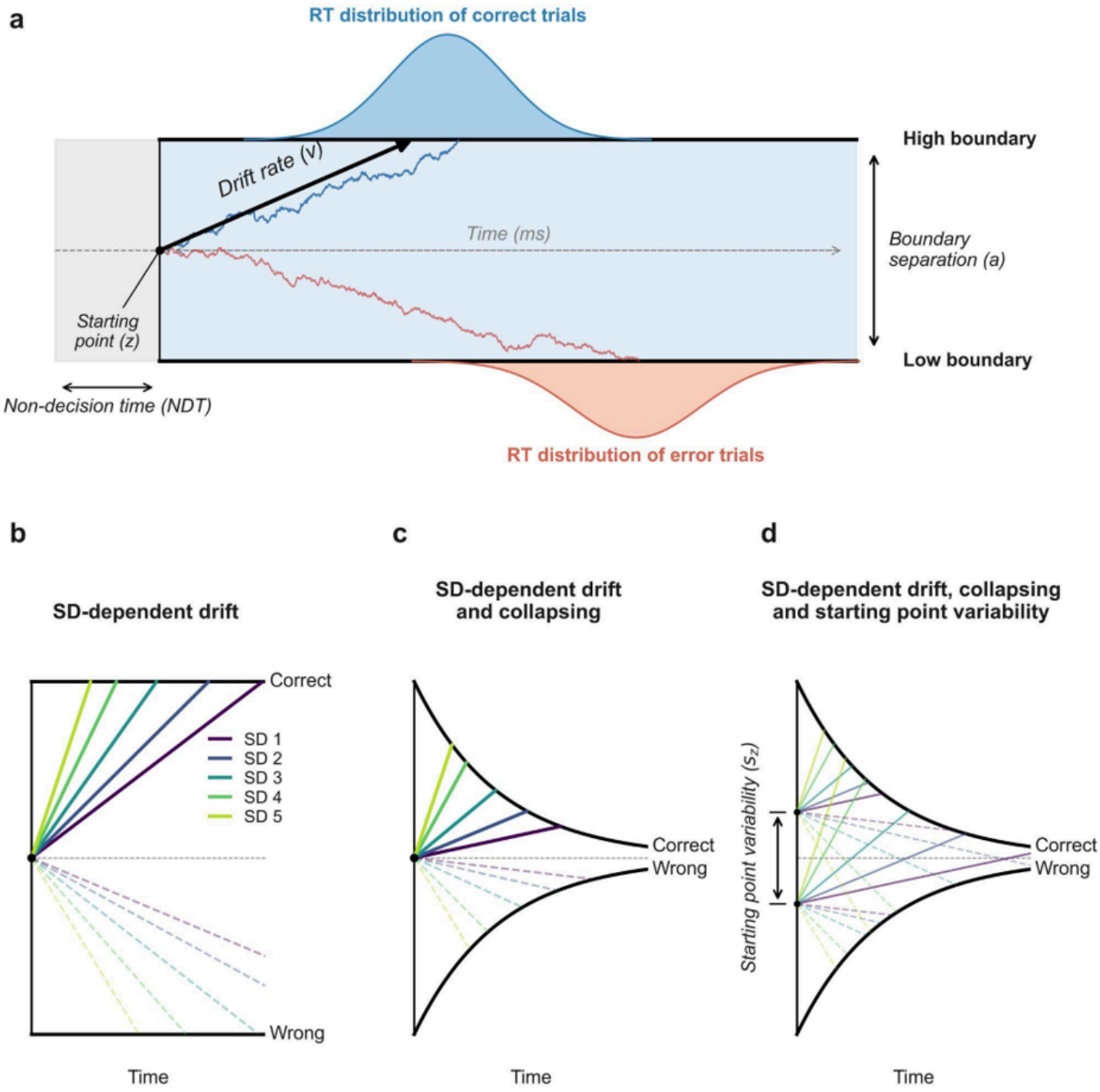


Figure 2

Drift Diffusion Model and its variants. a. The top panel shows the more realistic version of the model, including noisy evidence accumulation trajectories and the associated representative RT distributions. This panel also represents the null model, in which all parameters were held constant across SD. **b.** Stylized representations of the SD-dependent drift model; **c**. Stylized representations of the SD-dependent drift and collapsing model. **d**. Stylized representations of the SD-dependent drift, collapsing, and z variability model.

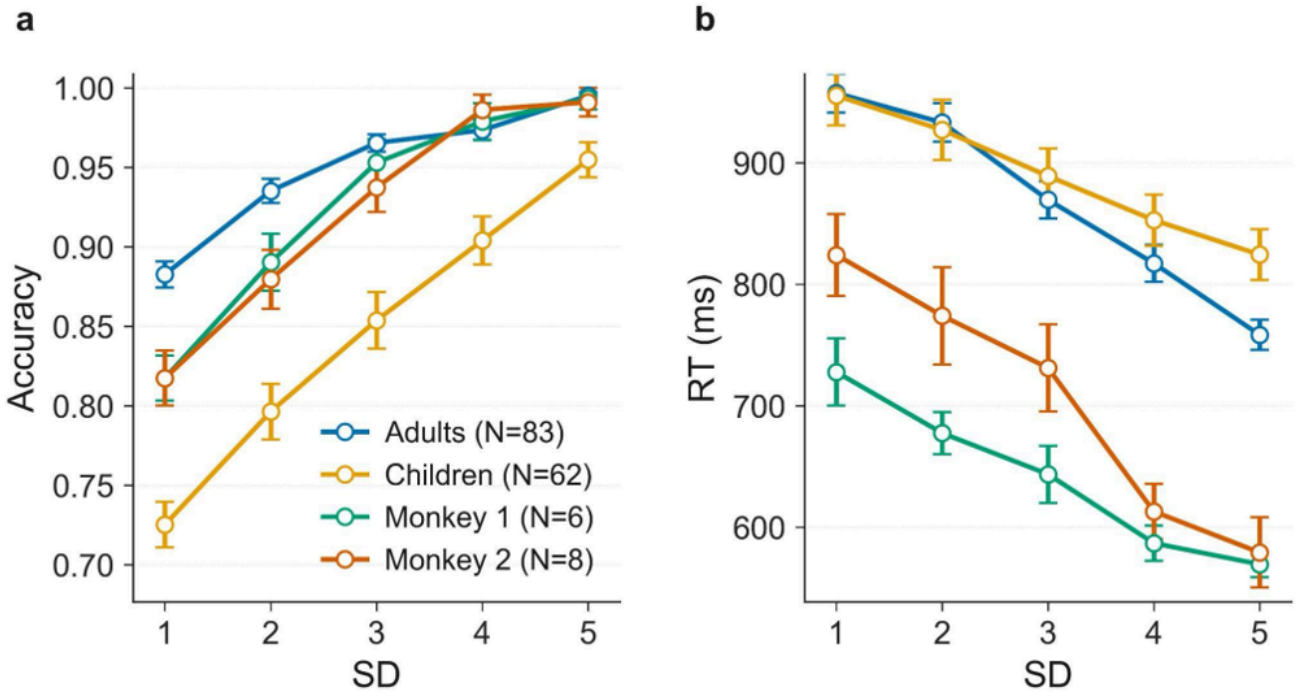


Figure 3

Cross-species behavioral strategies. a. Mean (± SEM) accuracy as a function of SD across groups. **b.** Mean (± SEM) RT as a function of SD across groups. N indicates the number of participants for Children and Adults groups and the number of sessions for the two monkeys.

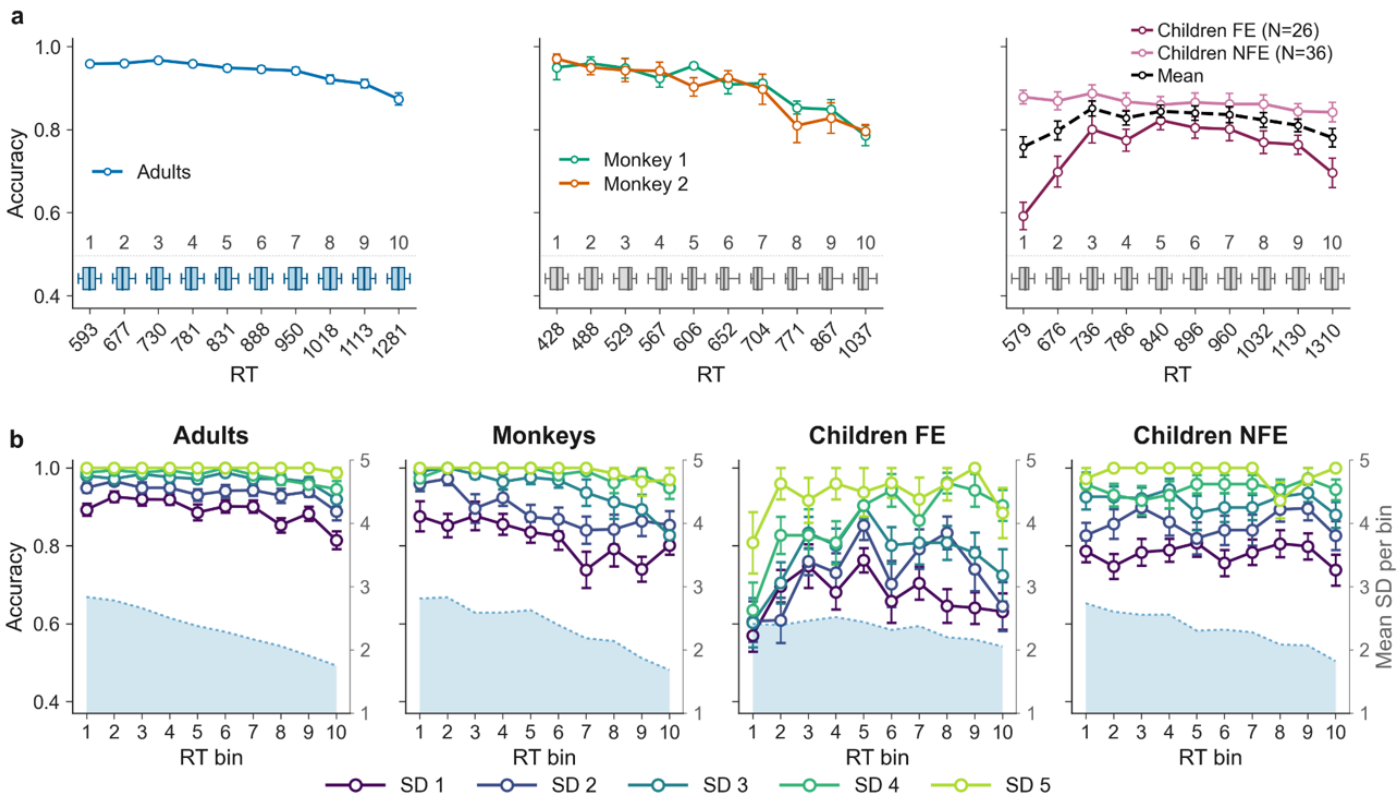


Figure 4

Differences in the speed-accuracy relationship. a. Observed CAF for each group, showing mean (± SEM) accuracy across 10 RT percentiles. Boxplots below each panel display the RT distribution within each bin (median, interquartile range, and 1.5× IQR whiskers). **b**. Observed CAF for each group and each SD, showing mean (± SEM) accuracy across 10 RT bins. The shaded area represents the mean SD per RT bin.

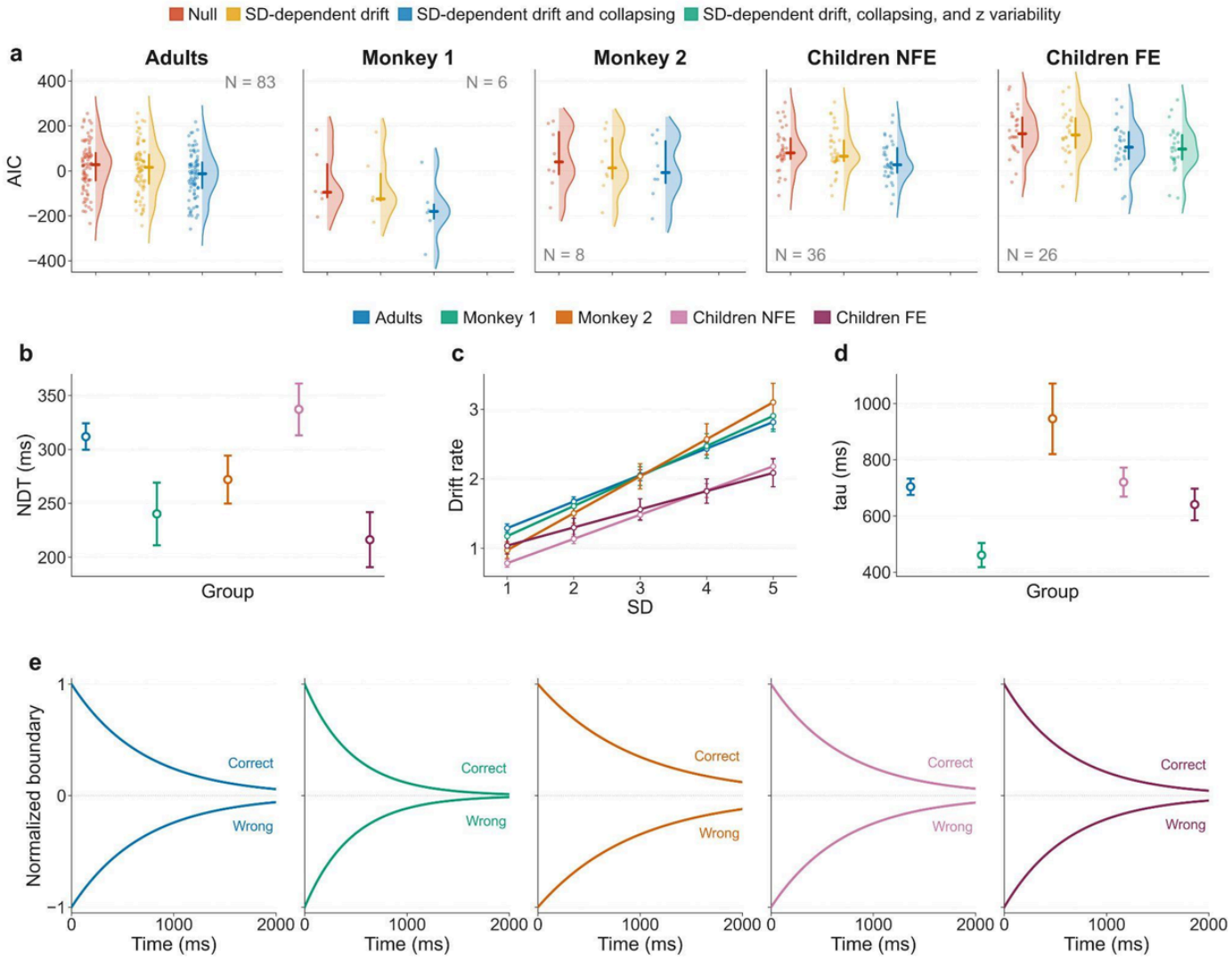


Figure 5

Drift-diffusion model comparison and parameter estimates across groups. a. Raincloud plots show the distribution of AIC values for the models fitted to individual subjects or sessions: the null model, the SD-dependent drift model, the SD-dependent drift and collapsing-boundary model, and, for the Children FE group, the SD-dependent drift, collapsing-boundary, and starting-point variability model. The half-violin plots represent the estimated distribution of AIC values, while each dot corresponds to an individual subject or, for the monkeys, an individual session. The vertical line indicates the interquartile range, and the horizontal segment indicates the median. Lower AIC values indicate better model fit. N denotes the number of subjects or sessions included in each panel. **b.** Mean (± SEM) NDT for each group. **c.**Mean (± SEM) drift as a function of SD for each group. **d.** Mean (± SEM) tau for each group. **e.** Collapsing decision boundary as a function of time for each group, generated using each group's mean tau. All curves were normalised to start at 1 for visualisation purposes only, to highlight tau-dependent differences in the rate of boundary decay across groups.

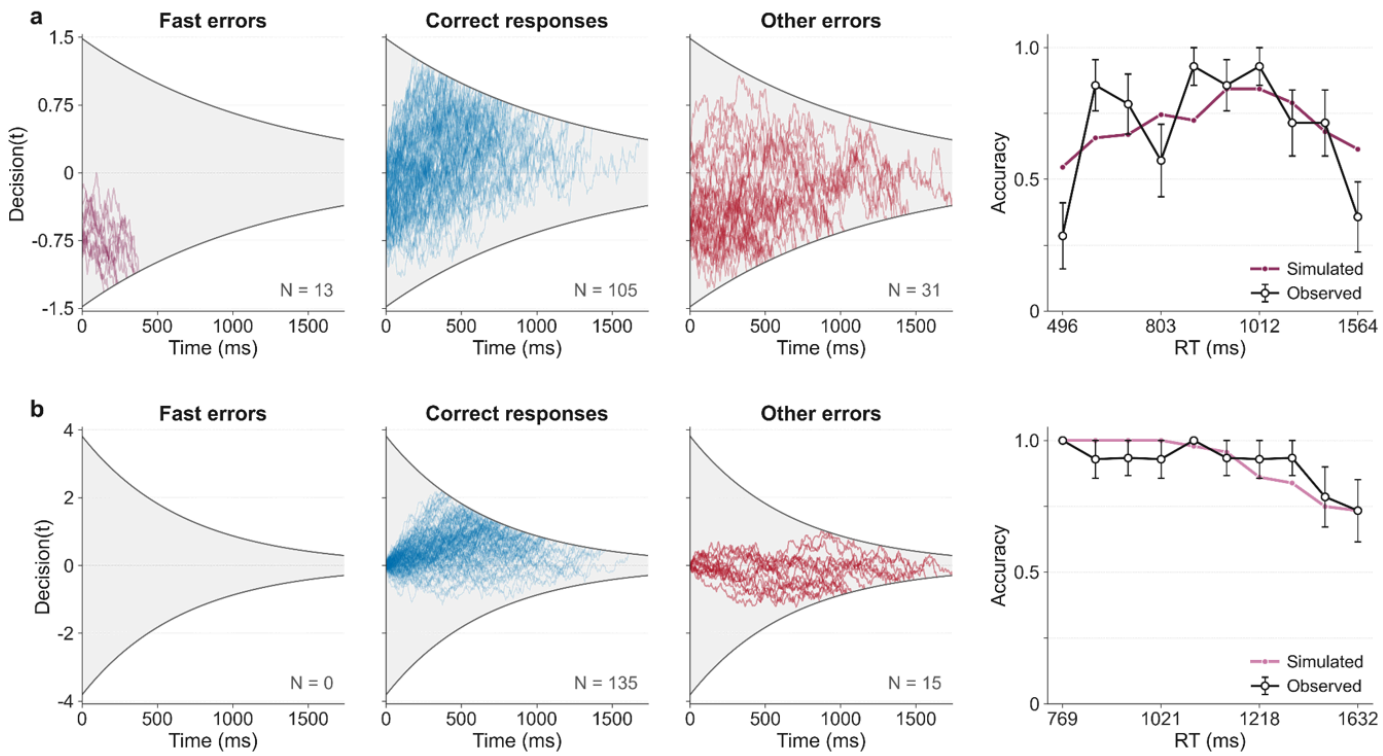


Figure 6

Latent DDM trajectories in two example subjects with different best-fitting models. a. Example of a subject with SD-dependent drift, collapsing, and z variability as the best model. **b.** Example of a subject with the SD-dependent drift and collapsing model as the best model, shown with the same three-panel layout and the same bin-based error classification. Both panels show decision-variable trajectories over time for fast errors, correct responses, and other errors. Noisy lines show single-trial trajectories, and black curves indicate the collapsing decision boundaries. Errors were classified using the same equinumerous RT bins as the CAFs (10 bins): fast errors were error trials falling in the two fastest RT bins, and other errors were the remaining error trials. The rightmost panel shows the simulated and observed CAFs across the 10 RT bins, where colored lines indicate simulated data and black lines indicate the subject's empirical data.

Supplementary Files

This is a list of supplementary files associated with this preprint. Click to download.

- SegretietalSupplementary.pdf